

AN ABSTRACT OF THE THESIS OF

DEWEY A. MURDICK, JR. for the MASTER OF SCIENCE
(Name of student) (Degree)

in Chemistry presented on February 6, 1973
(Major) (Date)

Title: THE DESIGN OF AN EASILY OPERATED DC ARGON
PLASMA ARC FOR ATOMIC SPECTROSCOPIC ANALYSIS

Redacted for privacy

Abstract approved: _____
Edward W. Piepmeier

A long path dc plasma arc operated in an atmosphere of argon is described. The arc is easily ignited and operated, and is inexpensive to use. Samples were introduced into the arc as solution aerosols. Radially resolved emission measurements are reported for calcium, copper, and hafnium. The detection limit for hafnium, an element known to readily form oxides in flames, is 15 times better than emission and 10 times better than atomic absorption detection limits reported for chemical flames. Detection limits for calcium and copper were 0.01 ppm and 0.06 ppm respectively. Interference of phosphate on calcium was found to exist only in the cooler regions of the arc.

The Design of an Easily Operated dc
Argon Plasma Arc for Atomic
Spectroscopic Analysis

by

Dewey A. Murdick, Jr.

A THESIS

submitted to

Oregon State University

in partial fulfillment of
the requirements for the
degree of

Master of Science

June 1973

APPROVED:

Redacted for privacy

Assistant Professor of Chemistry
in charge of major

Redacted for privacy

Chairman of Department of Chemistry

Redacted for privacy

Dean of Graduate School

Date thesis is presented 6 February 1973

Typed by Opal Grossnicklaus for Dewey A. Murdick, Jr.

TABLE OF CONTENTS

| | |
|-----------------------------------|----|
| INTRODUCTION | 1 |
| INSTRUMENTATION | 5 |
| The Arc Chamber | 5 |
| Electrodes | 8 |
| Operating the Arc | 12 |
| Nebulizer | 14 |
| Spectrometer Observation System | 16 |
| Reagents | 18 |
| RESULTS AND DISCUSSION | 21 |
| Background Signal | 21 |
| Positional Scans | 23 |
| Phosphate Interference on Calcium | 30 |
| Calibration Curves | 30 |
| CONCLUSIONS | 35 |
| BIBLIOGRAPHY | 37 |

LIST OF FIGURES

| <u>Figure</u> | | <u>Page</u> |
|---------------|---|-------------|
| 1. | Drawing of a simplified cross section of the arc. | 6 |
| 2. | 1:1 Cross sections of the plasma arc. | 7 |
| 3. | Photographs of the electrodes. | 10 |
| 4. | Operating plasma. | 13 |
| 5. | Drawing of the nebulizer. | 15 |
| 6. | Diagram of the total system. | 17 |
| 7. | Locations for positional scans in the arc. | 19 |
| 8. | Background emission. | 22 |
| 9. | The effect of current on 50 ppm copper. | 24 |
| 10. | Positional scans for copper. | 27 |
| 11. | Positional scans for calcium and hafnium. | 28 |
| 12. | Hafnium calibration curve. | 31 |
| 13. | Copper calibration curve. | 32 |

THE DESIGN OF AN EASILY OPERATED DC ARGON PLASMA ARC FOR ATOMIC SPECTROSCOPIC ANALYSIS

INTRODUCTION

Because chemical flames have been easy to operate, relatively inexpensive, and are able to atomize samples injected as solution aerosols, they have been over the years the workhorse of spectroscopic analysis. Chemical flames are, however, limited to a useful range of from 1700° to 3500° K with some less common flames reaching as high as 5000° K. In part, alternatives to chemical flames have been sought because of the temperature limitation and of the need to increase atomization efficiency of the spectroscopic sample.

Various plasma discharge devices have been investigated as alternatives. Most of these devices fall into three categories: Induction-coupled plasmas, plasma jets, and modifications of the dc arc.

The induction-coupled plasma was first described by Reed (1) in 1961. It consists of a few turns of water cooled tubular copper coiled around a quartz tube. The copper coil is connected to an induction heating power generator operated at a frequency in the megacycle range and at a power of 2-5 kW. While one end of the quartz tube is open to the atmosphere, the gas and the sample to be analyzed are introduced at the other end (2). Dickensen and Fassel (3)

found that by increasing the frequency of the discharge they were able to create a toroidal shaped induction-coupled plasma. This configuration presented less resistance to the injection of aerosols into the inner regions of the plasma. They gave the detection limits for 26 elements for this induction-coupled plasma. For most of the 26 elements the plasma emission gave a better detection limit than the detection limits cited for flame emission and atomic absorption.

The plasma jet was first introduced in 1957 by Giannini (4). In 1959, Margoshes and Scribner (5) in the United States, and Korolev and Vainshtein (6) in Russia, independently published similar designs of the dc plasma jet for use as an emission excitation source for solution analysis.

A plasma jet is a flow of partially ionized gas that is forced to stream out of a small orifice at high velocity. This gas stream has a flame-like appearance and usually derives its high temperature from a dc discharge (2, p. 204).

The small orifice utilized the thermal pinch effect, first developed by Gardien and Lotz (7), to stabilize the discharge and control the current density in the arc. The spectroscopic analysis takes place in the stream of high temperature gases. In the literature the term, plasma jet, is often used loosely whenever a thermal pinch effect is used to stabilize a dc discharge. Valente and Schrenk (8) designed a dc plasma jet and gave detection limits for 12 elements. In most cases these detection limits were better than those cited for flame

emission or for atomic absorption.

Many of the literature citations of the plasma jets could be more accurately termed modifications of the dc arc. The definition used here of the modified dc arc is: A plasma in which the analysis is always done in the plasma region that is located between the two electrodes. The arc may or may not be thermal-pinch stabilized. Hence, Owen's (9) plasma jet, Valente and Schrenk's (8) plasma jet, and commercial plasma jets such as SpectraMetrics' SpectraJet (10) may be termed modifications of the dc arc. Two recent modifications of the dc arc were made by Marinkovic and Dimitrijevic (11) and by Marinkovic and Vickers (12). Marinkovic and Dimitrijevic were able to reduce to 3100° K the temperature of a stabilized dc arc operated in an atmosphere of argon by the addition of potassium chloride as a buffer. This lower temperature argon arc was found to improve the detection limits on the more easily ionized elements i. e., alkali metals and alkaline earths. Hydrocarbons were added to the argon atmosphere of the Marinkovic and Vickers arc to create a reducing atmosphere for the determination of aluminum and tungsten by atomic absorption. The results for the two arcs gave detection limits in most cases comparable or better than those for chemical flames.

Temperatures cited for induction-coupled or dc discharge type plasmas range from 2400° to 15,000° K (10). Temperature

measurements for free burning arcs in an argon atmosphere operated at a current of ten amperes yield temperatures of from 9000° to $10,000^{\circ}$ K (12). Because these high temperature plasmas are capable of emitting spectral lines which cannot be excited in the flame (2), the literature places more emphasis on atomic emission than on atomic absorption.

This thesis describes a new modification of a dc plasma arc operated in an atmosphere of argon. The goals of this modification were simplicity of design, ease of ignition, and ease of operation. Of particular interest was the determination of hafnium. Hafnium forms a stable oxide with a dissociation energy greater than 7 eV (3). It was hoped that this modification of the arc would give lower detection limits than those cited for flames. Results are given for the determination of calcium, copper, and hafnium, and for the interference of phosphate on calcium.

INSTRUMENTATION

The Arc Chamber

A cross section of the argon plasma arc is schematically shown in Figure 1. Detailed drawings are presented in Figure 2. The arc consists of two sections--a moveable upper arc chamber, and a stationary electrode holder. The arc chamber consists of two water-cooled brass segments, A1 and A2, with a pyrex cylinder, B, held between them with the four plastic bolts. The pyrex cylinder is coaxial with the arc. The pointed electrodes, I1 and I2, enter the arc chamber through the 3/8" diameter by 7/8" long hollow cylindrical pistons, E1 and E2. E1 and E2 are machined as part of A1 and A2. These pistons slide up and down within 3/8" cylinders machined in F1 and F2. The tolerance between each piston and its holder is only 0.00075" to minimize the contamination of the argon atmosphere by nitrogen and oxygen.

The electrode holder section consists of four brass segments--two electrode holders, H1 and H2, and two cylinder blocks, F1 and F2. Between the electrode holders and the cylinder blocks are cemented with alpha cyanoacrylate (Vigor #CE-476, Toagosei Chemical Industry Co., Ltd.) two 1/16" thick Bakelite strips, G1 and G2, which provide electrical insulation between the electrode holders and

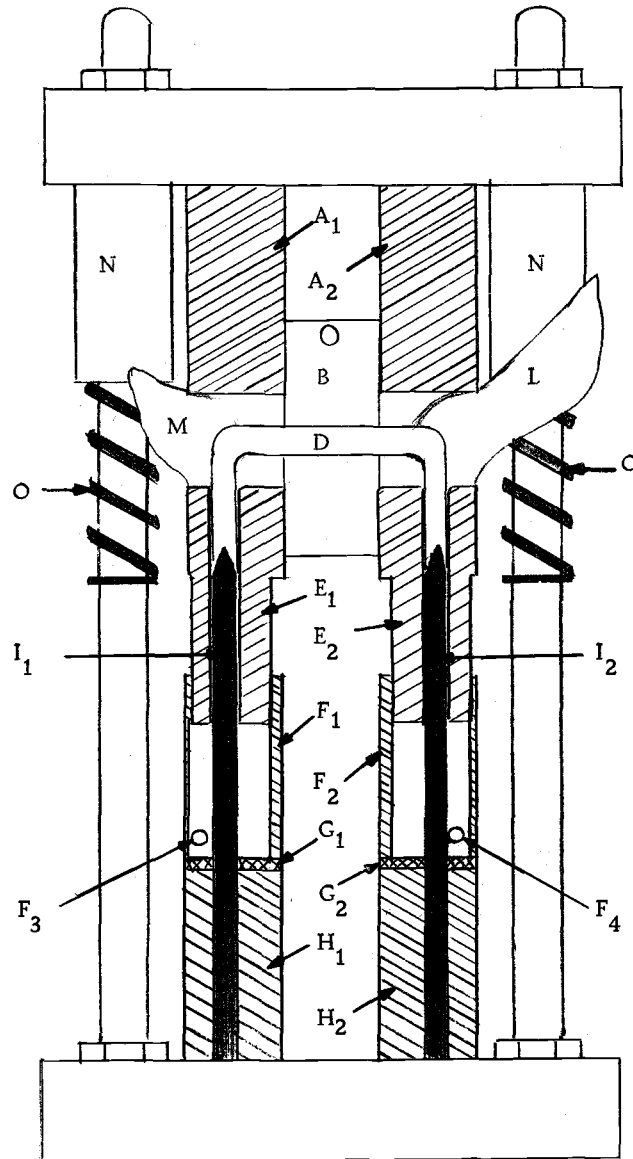


Figure 1. 1:1 drawing of a simplified cross section of the arc. More detailed drawings in Figure 2. Picture of the operating arc in Figure 4.

- | | |
|----------------------------|-------------------|
| A. Brass segments | I. Electrodes |
| B. Pyrex cylinder | L. Anode plume |
| D. The arc | M. Cathode plume |
| E. Hollow pistons | N. Guides |
| F1, 2. Cylinder blocks | O. Springs |
| F3, 4. Argon channels | P. Alignment rods |
| C. Bakelite insulation | |
| H. Brass electrode holders | |

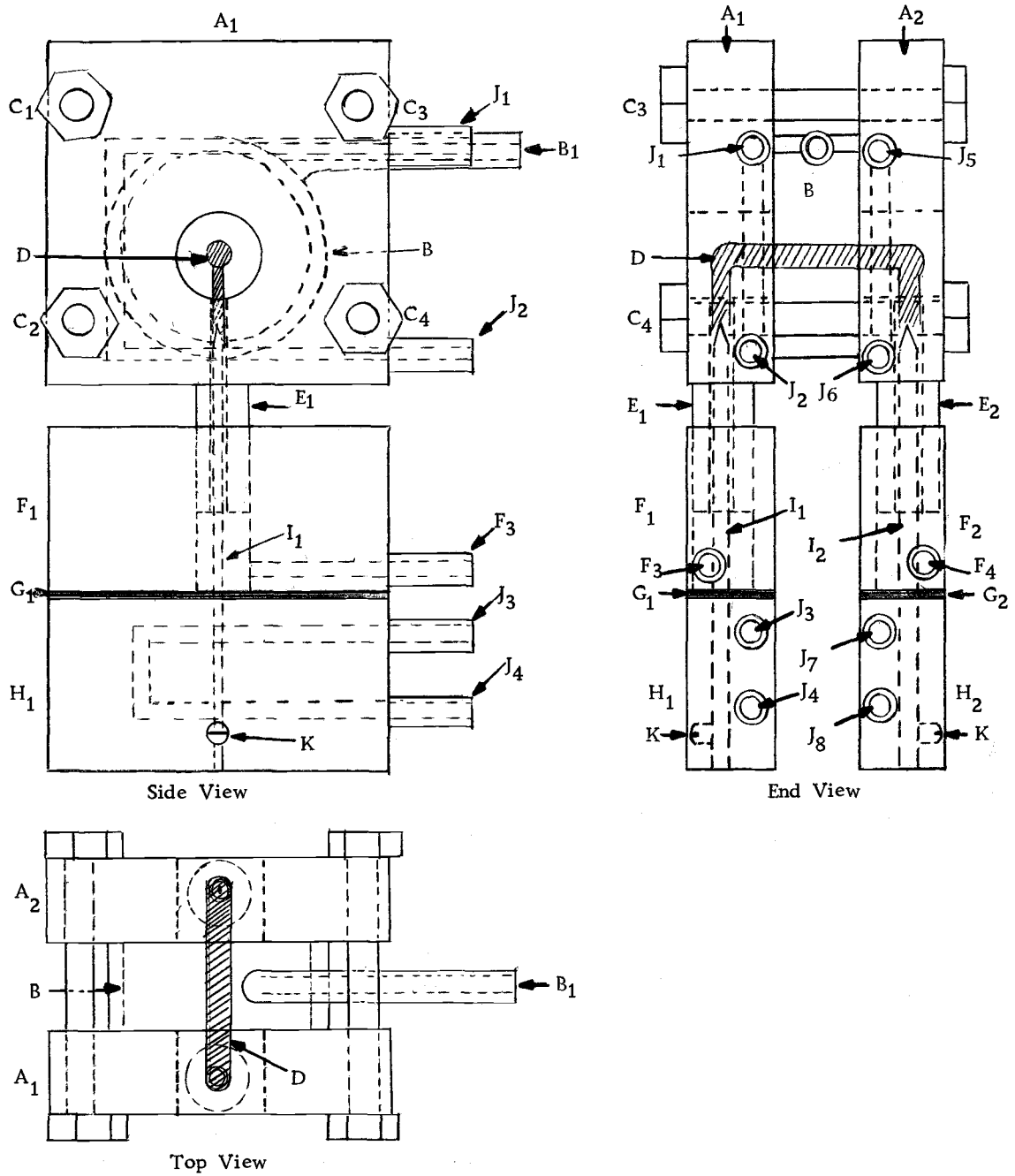


Figure 2. 1:1 Cross sections of the plasma arc (without housing).

- | | |
|------------------------|---------------------------------|
| A. Brass segments | G. Bakelite insulation |
| B. Pyrex cylinder | H. Brass electrode holders |
| C. Plastic bolts | I. Electrodes |
| D. The arc | J. Water channels |
| E. Hollow pistons | K. Set screw to hold electrodes |
| F1, 2. Cylinder blocks | |
| F3, 4. Argon channels | |

the rest of the device. All brass segments except the electrode holders float electrically to prevent arcing to them.

About 0.5 liters/minute cold water is run in a constant stream through J1-J8 (in that succession), Figure 2, to help remove the up to 600 watts of heat created in the arc chamber.

Argon is tangentially introduced at F3 and F4. The pistons, E1 and E2, move up and down in F1 and F2 to provide access to the tips of the electrodes for the purpose of igniting the arc. After ignition the electrode tips are allowed to recede out of the optical path.

Electrodes

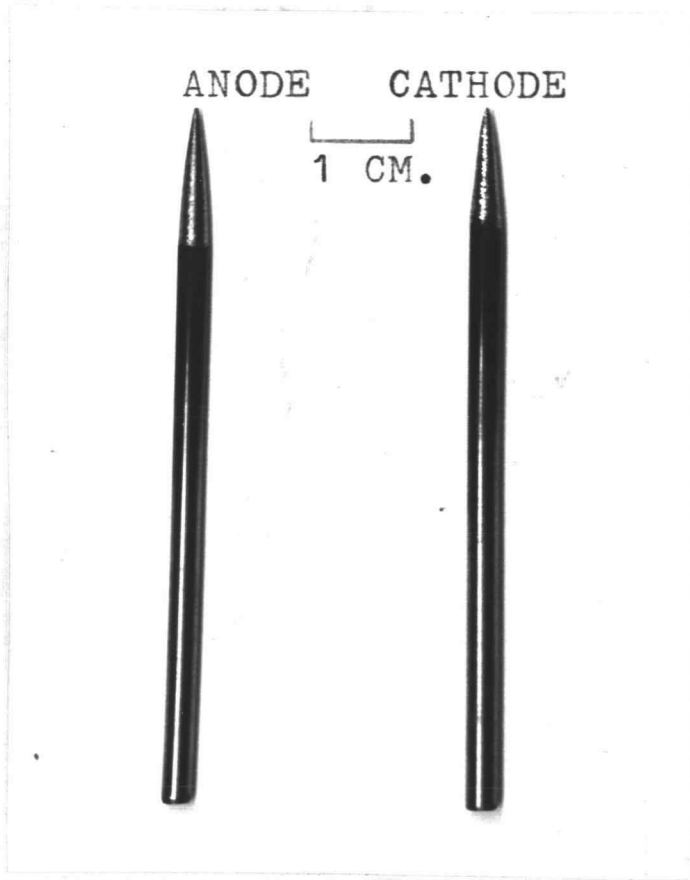
The arc burns between the two 1/8" diameter thoriated tungsten electrodes (2% THOR-TUNG ELECTRODES, Air Reduction Company, Inc., New York, N. Y.) in the channel indicated in Figure 1. The space around the electrodes in the cylinders, E1 and E2, is 0.031" to minimize arc wandering. The electrodes are continually bathed and cooled with a 0.5 liter/minute argon stream entering at points F3 and F4, Figure 1, which serves to minimize the consumption of the electrodes and lowers the voltage drop across the arc. Flow rates less than 0.5 liters/minute cause the electrodes to heat excessively while flow rates of 2 or more liters/minute cause distortion of the plasma. The arc can be blown out if flow rates of

five liters/minute or larger are used to flush the electrodes.

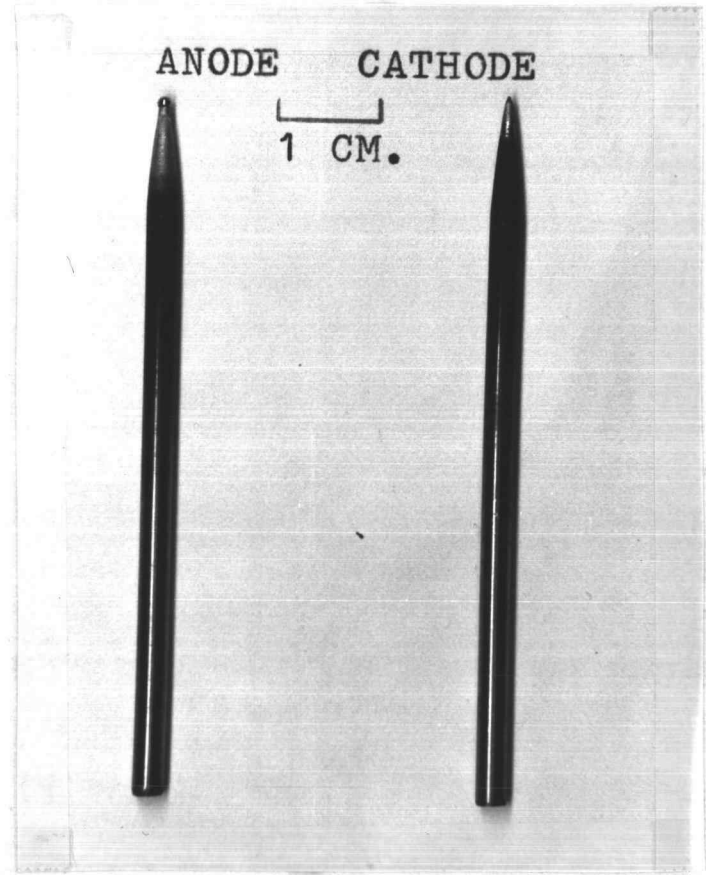
The removable electrodes are sharpened to a pencil-like point with a total angle of 14 degrees. The cathode retains its sharpness while the anode forms a small globule at the apex of the electrode, Figure 3. Although this globule does not distort the arc, it does enlarge with time and it was our practice to remove it about every eight hours by resharpening.

If the electrodes are not kept fairly sharp or if the electrodes are placed too high in the cylinders, E1 and E2, a kind of sputtering occurs. This sputtering consists of bright flashes of light randomly occurring near the anode end of the arc. Because these flashes occur most often just after the electrodes have been resharpened, they are believed to consist of bits of dust and/or tungsten metal momentarily blown off the irregular surface of the electrode. These particles heat rapidly and as they enter the anode plume they react violently with the oxygen present causing flashes of light. As the smooth surface of the globule forms, the flashes occur less often. These flashes were readily discriminated against during quantitative measurements as discussed later.

An argon stream which carries the sample aerosol is introduced tangentially into the pyrex cylinder at B1, Figure 1, and assists in the positional stabilization of the one-inch long central core (D in Figure 1) of the arc. The arc has the lowest resistance to current



After sharpening



After 8 hours of use

Figure 3. Photographs of the electrodes used in the plasma arc.

when a flow rate of 1.8 liters/minute is used. However, flow rates of from 1 to 10 liters/minute may be used. The seals between the pyrex chamber and the brass end plates are sufficiently air tight and the flow of argon from the electrode chambers is such that once the arc is ignited the arc will continue to burn even without the tangential argon stream. Conceivably, a very low flow rate could be used to introduce the analyte and perhaps increase the residence time of the analyte atoms in the arc. A flow rate of 3.7 liters/minute was used because this particular nebulizer would not work at flow rates as low as 1.8 liters/minute. An increase in flow rate from 1.8 to 3.7 liters/minute causes the resistance of a typical arc to go from 4.9 ohms to 6.2 ohms, with no sample introduced at either rate. Nebulization of a sample containing 1000-ppm sodium caused the resistance to drop from 6.2 ohms to 6.0 ohms. The arc can be blown out with this argon stream at a flow rate above 10 liters/minute, above the range of the flow meter.

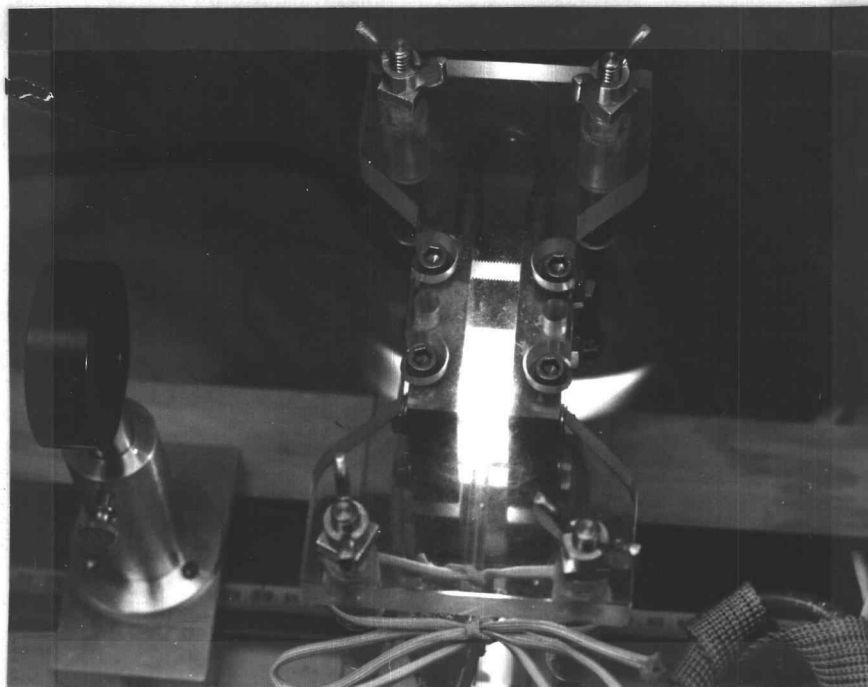
The power supply used for the arc, model PAK-16, (Electromatic Products Co., Chicago, Ill.) has an open circuit voltage of 105 volts. It contains selenium rectifiers. These rectifiers heat as an arc burn progresses and their resistance changes. Also, there is no fine current control on the power supply. A variable ballast resistor was placed in series with the arc to manually maintain a constant current. For most studies a current of nine amperes was

chosen. The resistor consisted of two, 2-ohm 300-Watt Ohmite variable resistors placed in parallel. Since the arc has a resistance in the neighborhood of six ohms this gave a current control range of 15%.

Operating the Arc

To ignite the arc, the cooling water, the argon streams, and the power supply are turned on in that order. Then the spring loaded arc chamber is lowered so that the electrode tips are visible. A short carbon rod with an insulated handle is inserted through the horizontal channel to establish electrical contact between the electrodes. When the arc has been struck the carbon rod is removed and the upper portion is allowed to move back to its original position. The arc now has an inverted U-shaped pattern, Figure 1. Out of both ends of the arc chamber the hot glowing gases form luminous plumes. Although both anode and cathode argon flow rates are the same, the anode plume is about two times larger than the cathode plume. This is the case even when the sample argon stream is off. Figure 4 contains pictures of the arc as seen from overhead and from the anode end of the arc.

Argon flows were regulated by means of a standard two-stage pressure regulator held at 20 p. s i. pressure, and dispersed by air flow regulators (type 3PA and 2SA Kontes, Berkeley, Calif.)



Overhead view



Anode side view

Figure 4. Operating plasma. Upper picture - overhead view with larger anode plume on right side. Lower picture - operating plasma from anode side.

controlling flows to the anode and cathode respectively. A Matheson flow regulator (tube size R-2-15-B) controlled the flow to the pyrex cylinder. Since all the flow meters were calibrated for air they needed to be corrected for argon. The correction factor is given by the following equation (13):

$$\text{Correction factor} = \sqrt{\frac{1}{\text{Specific gravity of gas}}} \quad (1)$$

The correction factor for argon equals approximately 0.85 at 20° C. All flow rates were multiplied by this factor.

Nebulizer

Solutions were sprayed into the main argon stream by use of a chamber type nebulizer, Figure 5. The nebulizer was constructed using a Beckman (#4020) total consumption burner attached to a Plexiglas tube 4 1/4" long by 3 1/2" in diameter with one set of baffles placed 2" and 3" from the tip of the burner.

The nebulizer consumed 1.9 ml/minute with an argon flow rate of 3.7 liters/minute at 20 p. s. i. At these conditions nebulization efficiency is 6%. Nebulization efficiency is the ratio of the amount of solution entering the arc to the total amount sprayed into the chamber. The amount entering the arc was found by measuring the difference between the amount sprayed and the amount retained

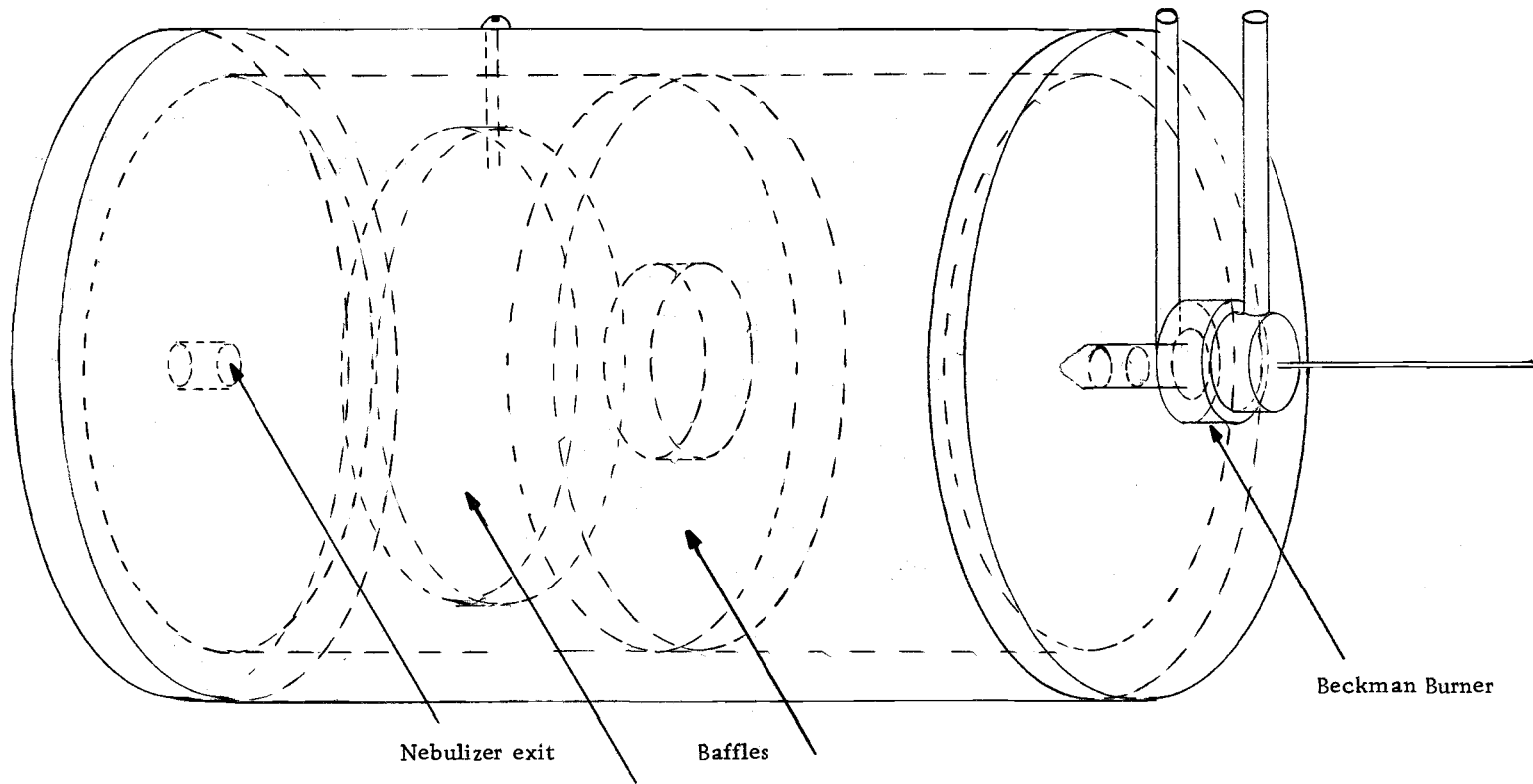


Figure 5. 1:1 image of the nebulizer as seen from an angle of 30°.

in the nebulization chamber.

The nebulizer is connected to the arc chamber by a 9" length of 3/16" ID Tygon tubing. There is some tendency for the fine aerosol to settle out on the tubing on the way to the plasma. This problem was solved by placing a small piece of heating tape along the tubing and heating moderately (25 watts).

Spectrometer Observation System

A block diagram of the total system may be seen in Figure 6.

Emission data were obtained using a McKee-Pedersen spectrometer station. The monochromator was equipped with a 15,000 line-per-inch grating blazed for 4000 \AA first order (reciprocal linear dispersion of 0.0037 nm/micron first order). In all studies cited in this paper a spectral band width of 0.1 nm was used. A 1P28 photomultiplier (in a McKee-Pedersen MP-1021 housing) was operated at -900 volts. The voltage for the photomultiplier was provided by a regulated dc power supply (MP-1002). The anodic current from the photomultiplier was converted to a voltage by means of a (MP-1031) chopper stabilized operational amplifier with a (MP-1009) high impedance selector set at 10^6 ohms, Figure 6. For all studies a time constant of 0.1 second was used. This time constant was short enough to allow spikes caused by the sputtering at the anode (discussed earlier) to be visually discriminated against for

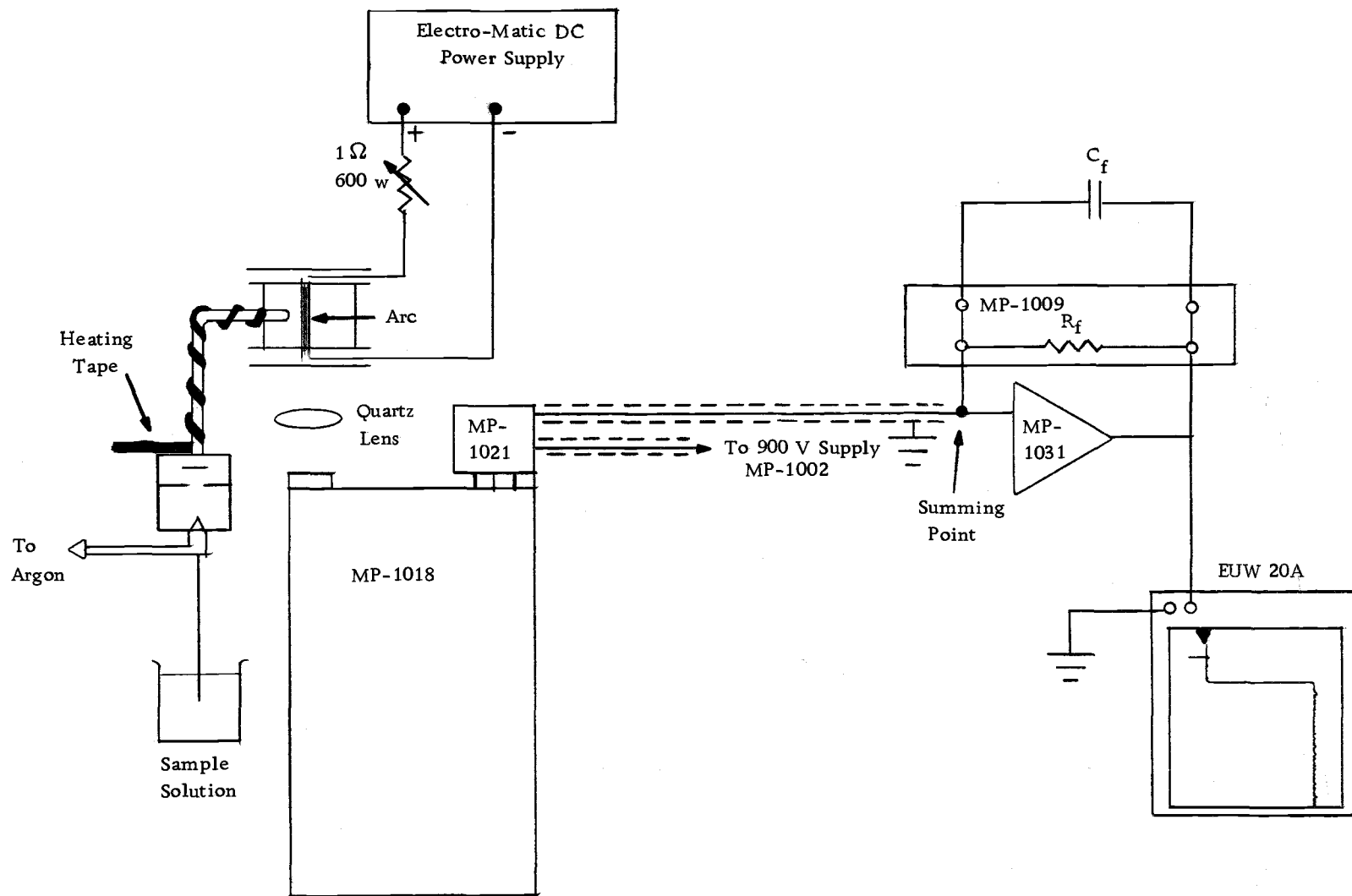


Figure 6. Diagram of total system (not drawn to scale).

quantitative measurements. The time constant is equal to the product of the feedback resistor, R_f , across the operational amplifier and the parallel feedback capacitor, C_f . The voltage was recorded using a Heath recorder (Model EUW 20A).

Emission measurements were made on the cathode side of the arc with the optical axis parallel to the horizontal portion of the inverted U-shaped arc, Figure 7. The reason for restricting the observation to the cathode end of the arc was that significant curvature of calibration curves occurred at high elemental concentrations, apparently due to self absorption, when the anode end was viewed. The electrodes and the vertical arc regions near the electrodes are not viewed by the monochromator. A one-to-one image of the center of the arc is focused with a 50-mm focal length quartz lens onto a 2-mm diameter aperture placed directly in front of the slits. The arc is mounted on a micrometer stage to allow a reproducible image of the arc to be moved transversely across the entrance of the slit.

Reagents

Standard dilutions from the stock solutions shown in Table 1 were used for all studies. All solutions were prepared with distilled water and were stored in polyethylene containers.

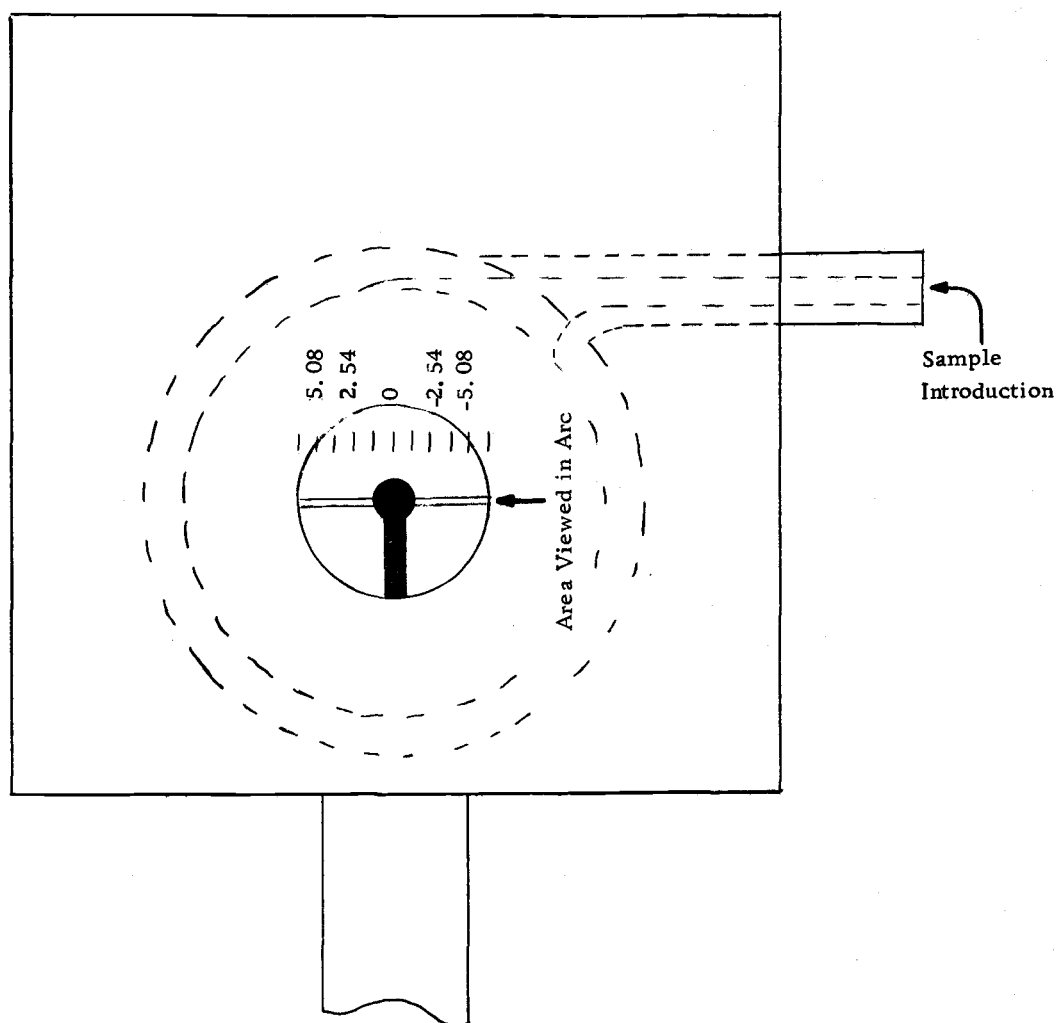


Figure 7. Locations in millimeters for positional scans in the arc.

Table 1. Reagents

| Desired Solution | Material Used | Diluted to |
|--------------------|---|------------|
| 1000 ppm copper | 7.859 grams of copper sulfate pentahydrate | 2 liters |
| 1000 ppm hafnium | 2.000 grams of the metal dissolved in 5 ml concentrated hydrofluoric acid | 2 liters |
| 1000 ppm calcium | 2.726 grams of calcium chloride dihydrate | 1 liter |
| 1000 ppm phosphate | 1.453 grams of potassium dihydrogen phosphate | 1 liter |

RESULTS AND DISCUSSION

Background Signal

Background emission of the arc operated at nine amperes, at a position of 2.86 mm from the center of the arc and at a wavelength of 324.75 nm is seen in Figure 8. Water was nebulized into the plasma at 0.1 ml/minute. At point A in Figure 8 is a spike caused by one of the flashes of light discussed in the Electrode section above. Neglecting point A, the noise on the signal was found to be within the limitations of shot noise for a photomultiplier. Over the five-minute period the arc was stable within the limits of shot noise.

The magnitude of the photomultiplier shot noise may be calculated from (14):

$$\frac{S}{N} = \frac{\sqrt{i_{\text{cathodic}}}}{\sqrt{2ef}} \quad (2)$$

Where:

- S = the intensity of the signal
- N = the RMS noise on that signal (peak to peak noise divided by five)
- i_{cathodic} = cathodic current of the photomultiplier
- = i_{anodic} / photomultiplier gain

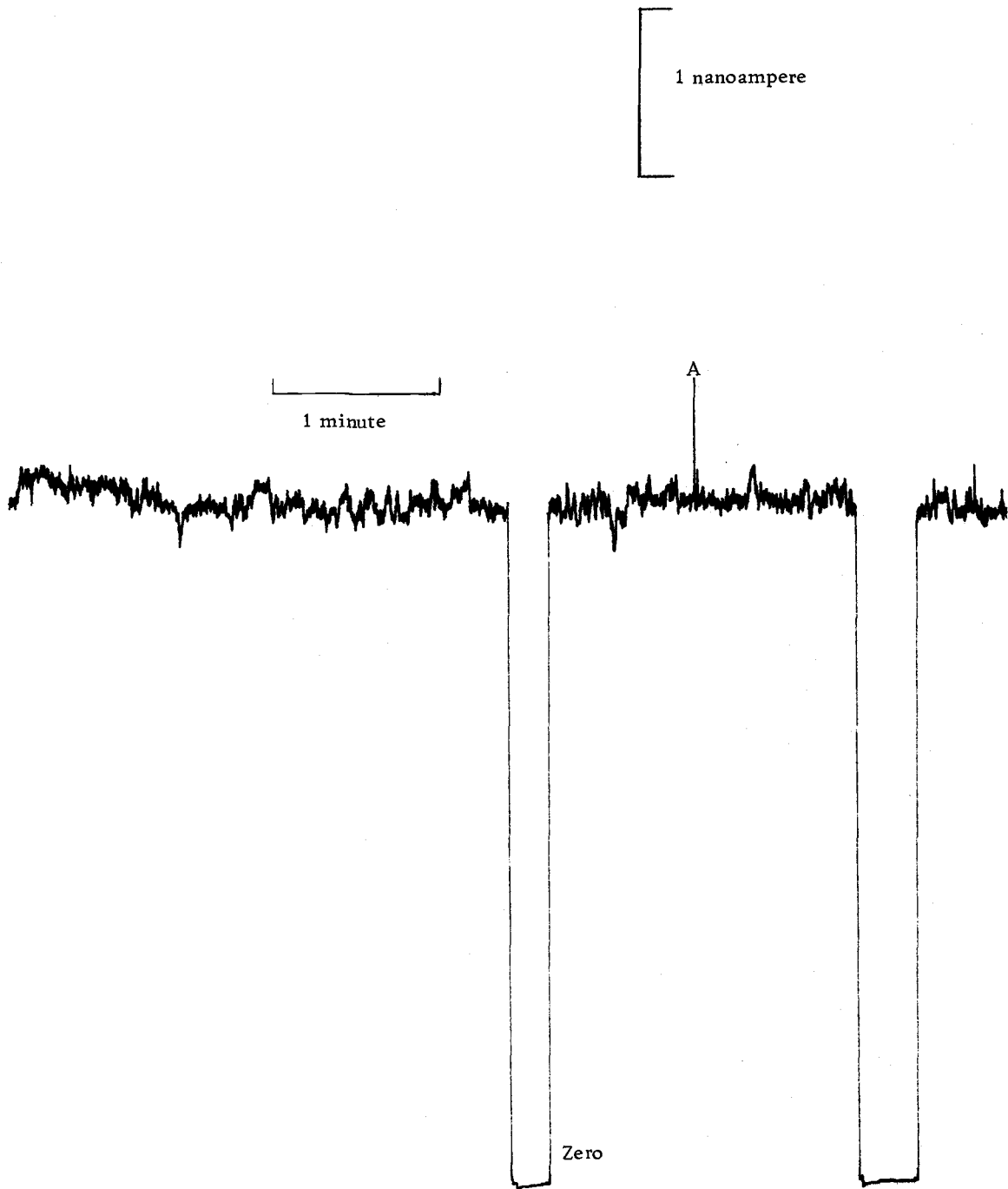


Figure 8. Background emission for a 9 ampere arc at 2.85 mm from arc center at 324.75 nm.

$$e = 1.60 \times 10^{-19} \text{ coulombs}$$

$$f = 1/4 R_f C_f \text{ where } R_f = \text{the feedback resistor across the operational amplifier}$$

$$C_f = \text{the capacitance of the parallel capacitor.}$$

Assuming the photomultiplier has a gain of 10^6 and that a time constant, $R_f C_f$, of 0.1 seconds is used, Equation 2 reduces to:

$$\frac{S}{N} = 1.1 \times 10^6 \sqrt{i_{\text{anodic}}} \quad (3)$$

From Figure 8, the background signal is observed to be 40.5×10^{-10} amperes. The peak to peak noise during a representative one minute interval is 3×10^{-10} amperes. The observed signal-to-noise ratio is, therefore, 67. From Equation 3 the signal-to-noise ratio is about 72. These values compare very favorably, considering the uncertainty in the value of the photomultiplier gain, and indicate that the major source of noise in this signal is shot noise.

Positional Scans

A horizontal section across the center of the arc was studied to determine the effect of arc current on an analytical signal. Figure 9 shows how the emission signal at 324.75 nm (corrected for background) varies with current and position for a 50-ppm copper sample. The background was observed with a water blank being nebulized at the same rate as the copper solution. The background

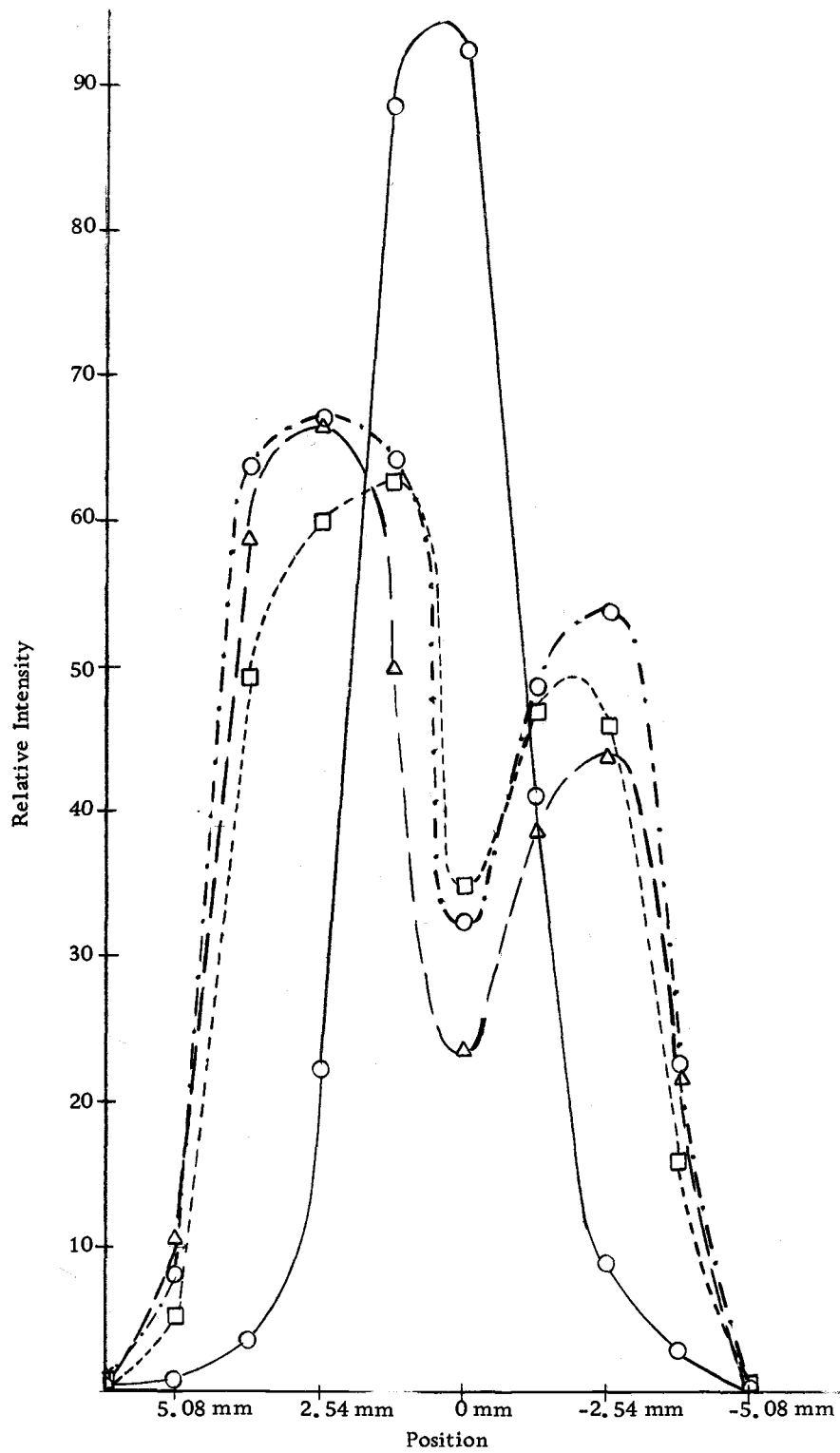


Figure 9. The effect of current on 50 ppm copper.
 - - - - □ 8 amp signal — — — — △ 10 amp signal
 - · - · - ○ 9 amp signal — — — — ○ 9 amp background

for the nine ampere blank is plotted for the purpose of comparison.

Figure 9 shows that increasing the arc current causes a decrease in the neutral atom analyte signal in the center of the arc. This inverse effect of current upon the signal is thought to be due to the direct relationship between current and the rate of collisions, which promote ionization in the plasma. Monatomic gas plasmas such as an argon arc operated at atmospheric pressure do not achieve local thermodynamic equilibrium under 15 amperes (2, p. 126, 127). A state of local thermodynamic equilibrium exists when the collisional rates are high enough that the average energy of the various groups of particles is the same within a localized region.

Below 15 amperes, where this arc is operated, a higher current apparently results in higher collisional rates, until 15 amperes where local thermodynamic equilibrium is reached. The higher the current, up to 15 amperes, the higher the collision rates and the greater the degree of ionization of the analyte atoms and the lower the signal from analyte neutral atoms.

A decrease in concentration of analyte atoms might also result from a decrease in total particle concentration that occurs when higher average energies cause gas expansion in a manner similar to that predicted by the ideal gas law for an open system at constant pressure.

Figure 9 shows that the arc is approximately symmetrical and that the positions from 6.35 mm to 0.00 mm have a higher S/B ratio than the positions from 0.00 mm to -6.35 mm. Because of this higher S/B ratio future studies were done in the region from 6.35 mm to 0.00 mm.

Figure 10 shows the study of 50 ppm copper and 5 ppm copper. The 5-ppm scan has a sharper emission peak than does the 50-ppm scan. This peak flattening for the 50-ppm scan apparently is not due to self absorption or self reversal because 50 ppm copper observed at a position of 2.86 near the center of this peak falls on a linear portion of a calibration curve. If self absorption were present at high concentrations a calibration curve would bend toward the concentration axis.

Figure 11 gives the results for a neutral atom line and an ion line each for the elements of hafnium and calcium. The concentration of calcium for both lines is ten ppm. The concentration of hafnium for both lines is 1000 ppm. The peak locations of maximum emission for both hafnium lines occurs at about 2.54 mm while the peak locations for the neutral atom line and the ion line for calcium are widely separated.

The locations of the peaks for the calcium ion line and the neutral atom line are thought to be explained by the competition of the calcium ion and neutral atom for the total available calcium in

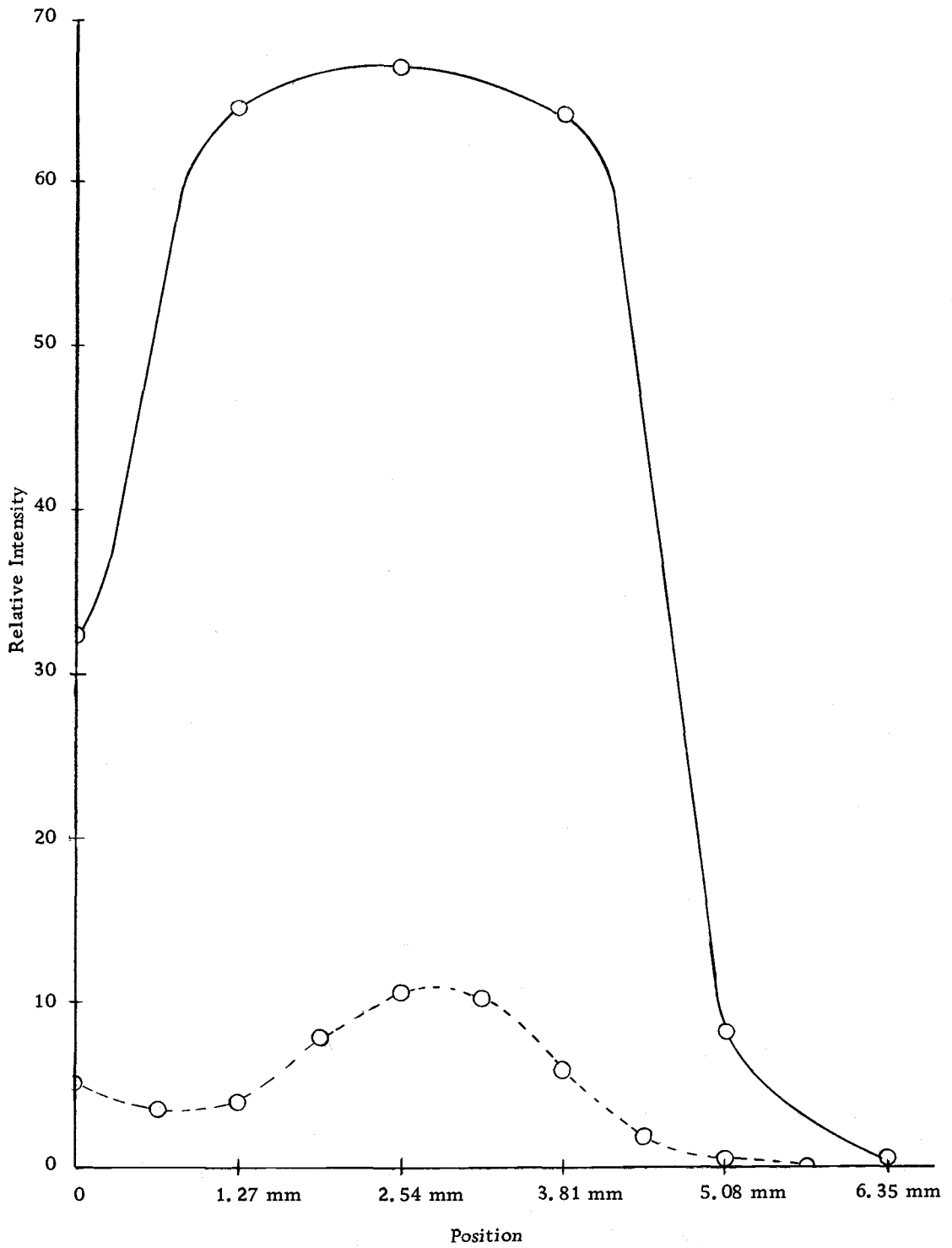


Figure 10. Positional scans at 9 amperes for 50 ppm (solid line) and 5 ppm (dash line) copper at the wavelength of 324.75 nm.

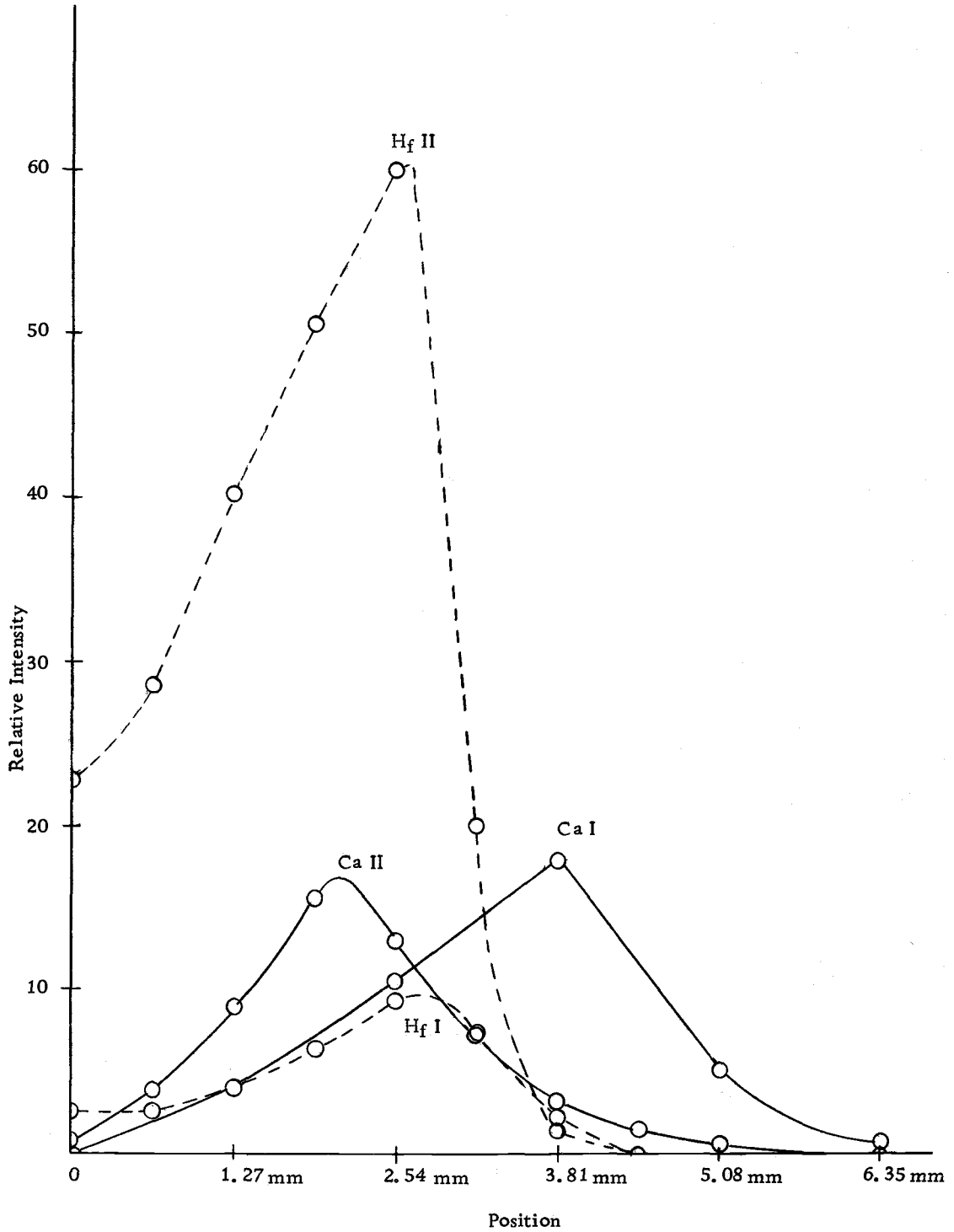


Figure 11. Positional scans at 9 amperes for 10 ppm calcium (solid lines) and 1000 ppm hafnium (dashed lines). Respective wavelengths are Ca I - 422.67 nm, Ca II - 393.37 nm, Hf I - 368.22 nm, Hf II - 339.98 nm.

the arc that has a large temperature gradient from its core to its outer regions. Temperatures attributed to free burning argon plasmas are in the range of 9000° to $10,000^{\circ}$ K (3, 10, 12). For the arc described in this thesis this temperature is assumed to exist only at the central core of the arc. The ionization of calcium, ionization potential 6.1 eV (15), takes place in the higher temperature region of the arc, near the center, while the calcium neutral atom line peaks in the cooler region of the arc. The calcium ion does not peak at the central core of the arc because the high temperatures present there create a calcium III ion with an ionization potential of 11.9 eV (15).

The coincidence of the position of the hafnium ion line peak with the neutral atom line peak is thought to be explained by a third competing factor. Hafnium is very reactive with oxygen forming a refractive oxide. The oxide is very stable having a boiling point of over 5000° C (15, p. B94).

Table 2. Dissociation Energy for Diatomic Oxides

| Oxide | Dissociation Potentials | Reference |
|-------|-------------------------|-----------|
| CaO | 3.9 eV | (16) |
| CuO | 4.9 eV | (16) |
| HfO | > 7 eV | (3) |

In the arc there is an appreciable amount of oxygen introduced in the form of water. Water vapor introduced in the form of the sample aerosol makes up about 3% of the plasma atmosphere. In the cooler regions of the arc this oxygen reacts with the hafnium neutral atoms forming HfO and effectively removing hafnium atoms. It is thought that if this oxygen were not present the peak location for the hafnium neutral atom line would be displaced towards the outer region of the arc.

Phosphate Interference on Calcium

A brief study on the phosphate interference of calcium was conducted. The concentration of calcium was ten ppm while the concentration of the phosphate was 40 ppm. The phosphate was found to suppress the emission of the 422.67 nm line of calcium in the cooler regions of the arc. At a position of 6.35 mm from the center of the arc phosphate reduced the signal by 25% while at a nearby position of 5.08 mm the reduction of the calcium line was only 2%. Apparently this arc is energetic enough to dissociate calcium phosphate except in the very outer regions.

Calibration Curves

Figures 12 and 13 give calibration curves for the hafnium 339.98 nm line and for the copper 324.75 nm line. The Oregon

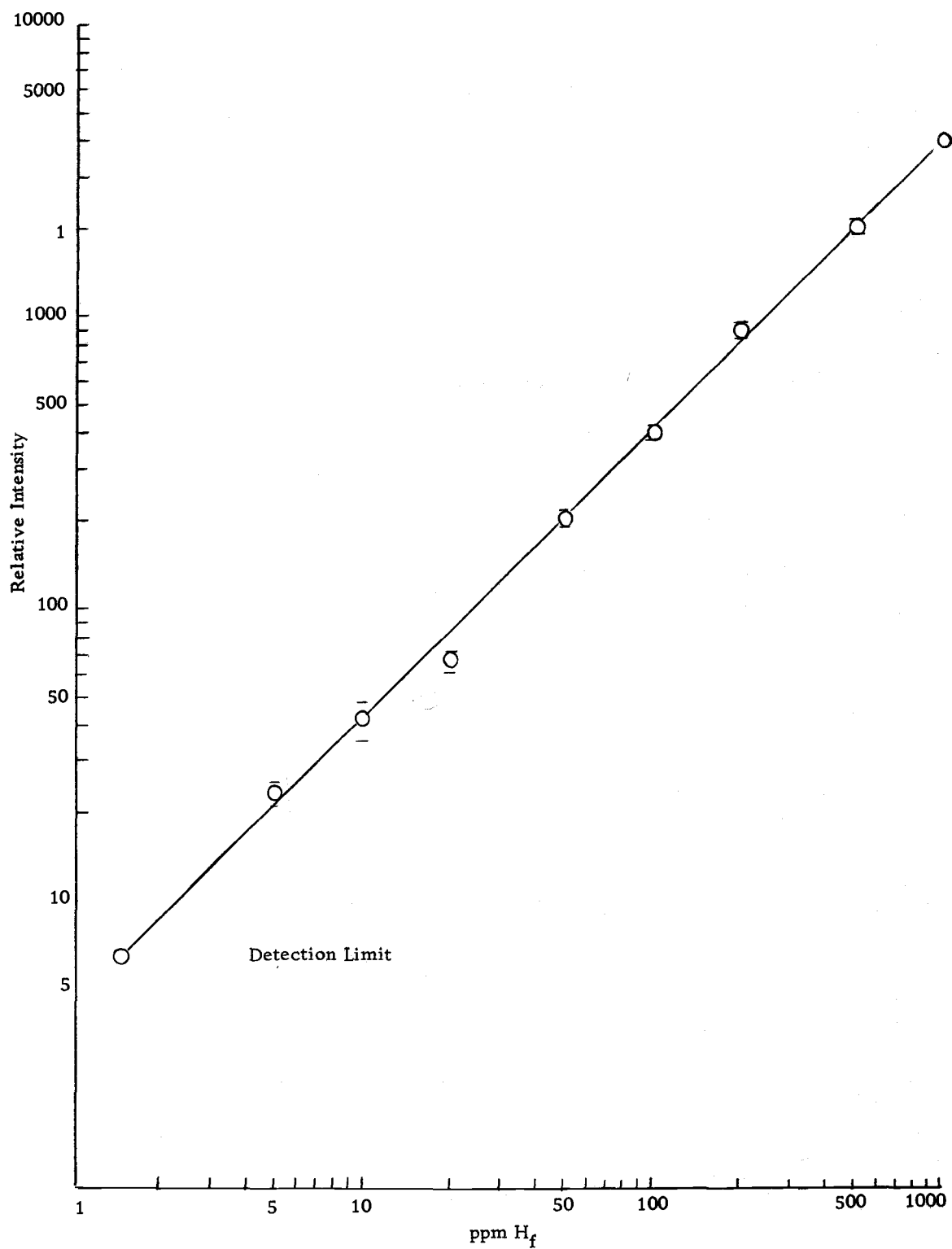


Figure 12. Hafnium calibration curve.

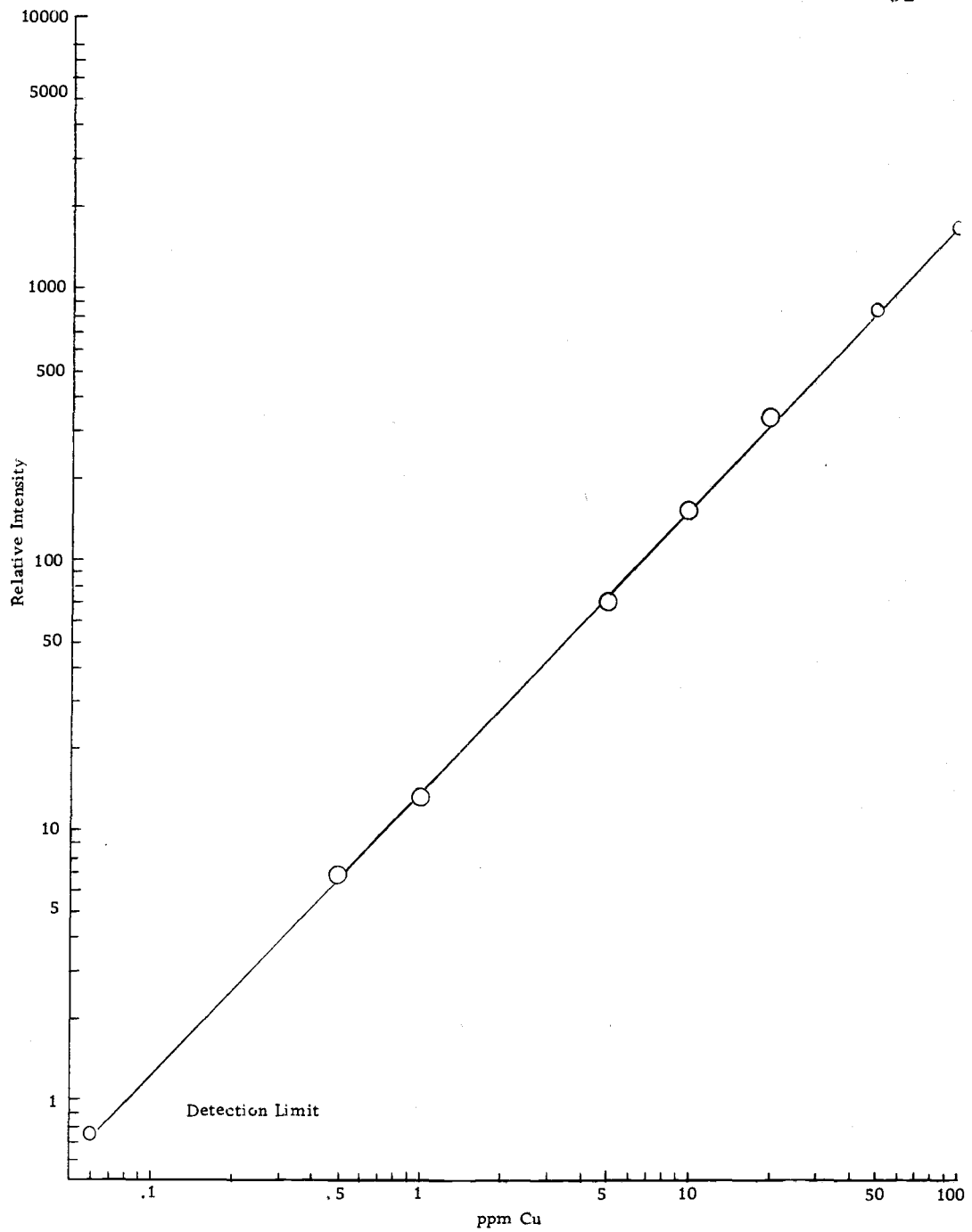


Figure 13. Copper calibration curve.

State University Computer Center program, *LINREG, gives a slope of $1.00 \pm .02$ and $1.04 \pm .01$ respectively for the log-log plots of concentration versus photocurrent. A slope of 1.00 indicates that the relationship between emission signal and concentration is linear and passes through the origin.

The detection limits for calcium, copper, and hafnium are shown in Table 3. Vickers and Winefordner's (17) definition of detection limit for chemical flames was used. The detection limit is the concentration of the element in solution which when aspirated into the plasma gives an emission signal equal to twice the standard deviation in the background measurement. The standard deviation was defined as 1/5 of the peak-to-peak noise value measured over a period of time equal to many time constants.

Table 3. Detection Limits ($\mu\text{g/ml}$)

| Element | Line in nm | Position in mm | Argon Plasma | Flame Emission (18) |
|--------------|---------------|-------------------|-----------------|------------------------|
| Calcium (II) | 393.37 | 1.90 | 0.5 | -- |
| (I) | 422.67 | 3.81 | 0.01 | 0.0001 |
| Copper (I) | 324.75 | 2.86 | 0.06 | -- |
| (I) | 327.40 | -- | -- | 0.01 |
| Hafnium (II) | 339.98 | 2.54 | 1.5 | -- |
| (I) | 368.22 | 2.54 | 6. | 75. |

There are at least two important factors other than the intensity of a line which affect the detection limits. The first is

the signal to background ratio. Figure 9 gives a representative background continuum for a 9-ampere burn. The emission from the center of the arc is very sensitive to minor current fluctuations. Therefore, as the position for observation of an analyte line moves in toward the center of the arc these fluctuations in the background emission can become a limiting factor. Thus, although Figure 11 shows the peak intensities for Ca I at 3.8 mm and Ca II to be about equal, the detection limit for the Ca II line at 1.9 mm is 50 times poorer than the detection limit for the Ca I line.

A second important factor is the effect of the spectral lines neighboring the line of interest. Although for a concentration of 1000 ppm the hafnium ion line is over six times as intense as the neutral atom line, Figure 11, its detection limit is only four times better than the detection limit for the neutral atom line. The ion line is in the region of the OH emission while the neutral atom line is found in a "spectrally clean" region of the arc.

CONCLUSIONS

The arc described in this thesis is stable and easy to operate. It can be used with the type of equipment found in many analytical laboratories. The arc was adequately stable even though a manually regulated power supply was used. A well regulated power supply would be an asset to further studies. The cost of operation of the arc is low, 75 cents/hour, compared to flames due to the low consumption of argon.

In this plasma arc the detection limit of copper, an element known to be relatively free of oxide formation in flames, is within the same order of magnitude as that reported for chemical flames. The detection limit for hafnium, an element known to readily form oxides in flames, is 15 times better than emission and 10 times better than atomic absorption detection limits reported for chemical flames.

The arc is sufficiently energetic that phosphate only interferes with calcium in the cooler regions of the arc.

Most of the recent papers on dc discharges in an argon atmosphere have an associated dehydrating system to remove most of the water vapor from the aerosol sample stream before it gets to the arc. This work showed that such a system was unnecessary for this arc. On the other hand it would be worthwhile to study the use

of such a system with this arc because it would reduce the available oxygen and might reduce oxide formation in the arc.

Because flow rates of the sample stream can be reduced to almost zero this arc is a good candidate for use with an ultrasonic nebulizer.

BIBLIOGRAPHY

1. Reed, T. B. Induction-Coupled Plasma Torch. *Journal of Applied Physics* 32(5):821-824. 1961.
2. Boumans, P. W. J. M. Excitation of Spectra. In: *Analytical Emission Spectroscopy, Part II*, ed. by E. L. Grove, New York, 1972. p. 191-204.
3. Dickinson, George W. and Velmer A. Fassel. Emission Spectrometric Detection of the Elements at the Nanogram per Milliliter Level Using Induction-Coupled Plasma Excitation. *Analytical Chemistry* 41(8):1021-1024. 1969.
4. Giannini, G. M. The Plasma Jet. *Scientific American*. 197(2):80-88. 1957.
5. Margoshes, M. and B. F. Scribner. The Plasma Jet as a Spectroscopic Source. *Spectrochimica Acta (Northern Ireland)* 15:138-145. 1959.
6. Korolev, V. V. and E. E. Vainshtein. The Use of a Plasma Generator as an Excitation Source in Spectrographic Analysis. *Journal of Analytical Chemistry U.S.S.R.* 14:731-735. 1959.
7. Gerdien, Von H. and A. Lotz. Über eine Lichtquelle von sehr hoher Flächenhelligkeit. *Zeitschrift für technische Physik* 4:157-162. 1923.
8. Valente, S. E. and W. G. Schrenk. The Design and Some Emission Characteristics of an Economical dc Arc Plasmajet Excitation Source for Solution Analysis. *Applied Spectroscopy* 24(2):197-205. 1970.
9. Owen, L. E. Stable Jet for Excitation of Solutions. *Applied Spectroscopy* 15:150-152. 1961.
10. Elliott, William G. A High Temperature Argon Plasma for Spectrochemical Analysis of Solid, Liquid, or Gaseous Samples. *American Laboratory*, August 1971, p. 45-52.
11. Marinkovic, M. and B. Dimitrijevic. Low-Temperature Arc as a Light Source for Emission Spectrometric Analysis of Solutions. *Spectrochimica Acta* 23B:257-264. 1968.

12. Marinkovic, M. and T. J. Vickers. Free Atom Production in a Stabilized dc Arc Device for Atomic Absorption Spectrometry. *Applied Spectroscopy* 25(3):319-324. 1971.
13. _____ Matheson Gas Products. General Catalog 28. p. 192. 1972.
14. Ingle, J. D., Jr., and S. R. Crouch. Critical Comparison of Photon Counting and Direct Current Measurements Techniques for Quantitative Spectrometric Methods. *Analytical Chemistry* 44(4):785-794. 1972.
15. Weast, Robert C. Editor-in-Chief. *Handbook of Chemistry and Physics*. 51st ed. Cleveland, The Chemical Rubber Co., 1970. p. E56.
16. Boumans, P. W. J. M. *Theory of Spectrochemical Excitation*. New York, Plenum Press, 1966. 383 p.
17. Vickers, T. J. and J. D. Winefordner. *Flame Spectrometry*. In: *Analytical Emission Spectroscopy, Part II*, ed. by E. L. Grove, New York, 1972. p. 333.
18. Slavin, Walter and Sabina Slavin. Recent Trends in Analytical Atomic Absorption Spectroscopy. *Applied Spectroscopy* 23(5): 421-432. 1969.